# Characterization and Optimization of Doped Polyaniline for Acetone Detection

**Raihana Bahru**

Institute of Microengineering and Nanoelectronics, Universiti Kebangsaan Malaysia,
43600 Bangi, Selangor, Malaysia
Corresponding author (e-mail: raihanabahru@ukm.edu.my)

Acetone, a group of volatile organic compounds (VOCs), harms the environment and human health. This work focuses on developing acetone detection materials for safety precautions. However, the main challenge of this type of gas sensor is the operation at high temperatures (greater than 200°C), which is barely practical for high-risk conditions. Therefore, this study proposes an attractive approach for designing sensing materials to operate at a lowered operating temperature by integrating an organic material as the additional sensing material. A conducting polymer known as polyaniline (PANI) was added to the titanium oxide ($TiO_2$) by in-situ chemical polymerization method to form the PANI-$TiO_2$ nanocomposite. The effect of doped PANI was studied in a range of percentage compositions. It was characterized using Field Emission Scanning Electron Microscopy (FESEM), Transmission Electron Microscopy (TEM), Fourier Transformation Infrared Spectroscopy (FTIR), and $N_2$ adsorption-desorption analysis. Meanwhile, the performances of composite pellets were measured at lower temperatures (below 70°C) for acetone concentrations of 100 – 500 ppm and optimized. It was found that 30 wt.% of PANI-$TiO_2$ was the best percentage loading, giving the maximum sensitivity. The optimum performance was obtained at 45°C of operating temperature with sensitivity approximately at 16.19% for 300 ppm of acetone exposure.

**Keywords**: Acetone; adsorption-desorption; conducting polymer; polyaniline

Urban air pollution is a major problem in a fast-developing country. Volatile organic compounds (VOC) are one of the classes targeted at solving air pollution and are commonly found in various applications in the industrial and research sectors. The sources of the emission that contributed to the higher amount are natural and anthropogenic (human-made) [1]. In safety measurement, the semiconductor-based sensor is one of the most preferable VOC sensors to counter the air pollution issues and approach to control the emission. Acetone vapour is in a group of VOC that is hazardous to society with can causes that present in the atmosphere and contribute to the air pollution problem. It is mainly found in pharmaceuticals, plastics, fertilizers, and synthetic applications, and it is dangerous when the emission exceeds 1 ppm [2]. Therefore, designing the sensors operated at lower vapor concentrations and temperatures is challenging.

Metal oxide semiconductor gas sensors, such as $TiO_2$ gas sensors, are well-established in commercial devices. Still, it faces many limitations, including high operating temperature (more than 200°C), less stability at lower temperatures, and less selectivity and sensitivity [3-5]. Therefore, the alternative approach is to incorporate the organic compounds into the inorganic gas sensor as a background to sustain stability and enhance detection sensitivity [6]. Kashyap et al. [7] reported that introducing conducting polymers such as polyaniline (PANI) can be operated at lower temperatures and possess good stability in longer detection. They detected toluene, and the sensor was stable for 45 days. In a neutral state, PANI is in the form of an emeraldine base and is less conductive. Thus, PANI will be further acidified in the chemical oxidation process by introducing acid, resulting in PANI emeraldine salt, as illustrated in Figure 1. The VOC molecules will interact with the polaron (positively charged) and bipolaron present in the PANI chain. This movement of polarons will affect the conductivity of the PANI chain, involve the donation and acceptance of electrons, and act as a p-type semiconductor gas sensor [7-8]. Many researchers are developing PANI-based gas sensors for safety precautions due to the superior properties of PANI besides good stability during detection [9-12].

This study developed $TiO_2$ acetone sensor materials by introducing various PANI loadings to form nanocomposites. The synthesis of PANI from its monomer, aniline, is done through oxidative polymerization. An ammonium persulfate (APS) acts as an oxidant to form emeraldine salt. The nanocomposites were characterised to observe the surface morphology, which is essential to the effectiveness of sensing activity. The effect of different loadings is
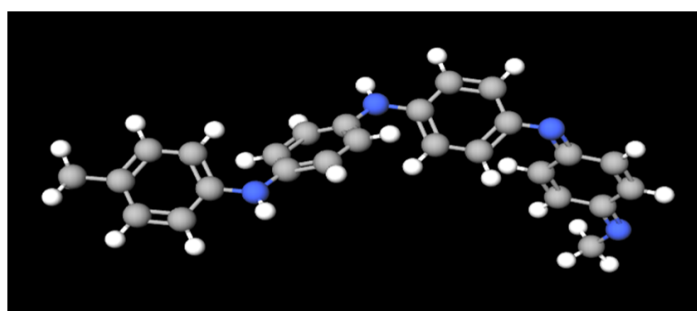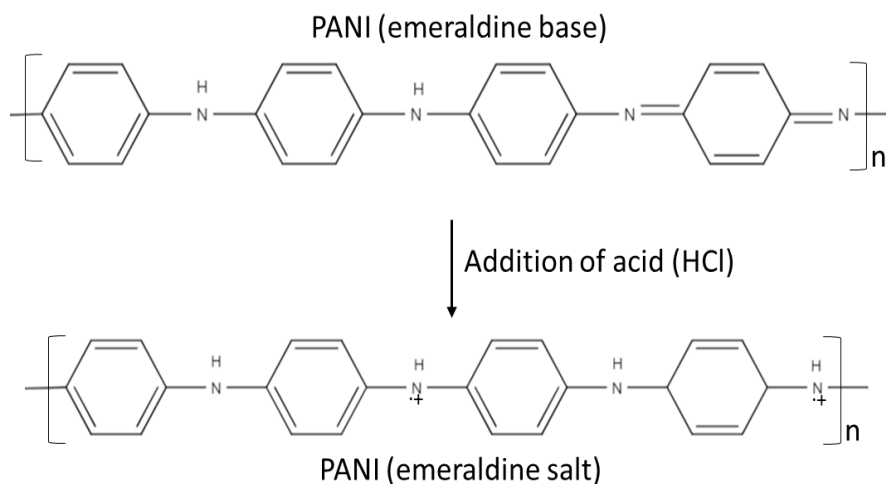
---

†Paper presented at the 4th International Conference on Recent Advancements in Science and Technology (ICoRAST2023)

**Figure 1.** Chemical structure of PANI in the form of emeraldine base and emeraldine salt. [Down] The illustration of the structure of PANI in 3 dimensional formation.

studied to see the materials' complementation and formations according to the suitable adsorption process, such as higher surface area and larger porosity. The optimization of the operating condition was also conducted, and the error of the percentage sensitivity was minimized by analysis using the response surface method.

## EXPERIMENTAL

### Chemicals and Materials

The chemicals used were aniline (analytical reagent grade, purity > 99%, Fisher, United Kingdom), ammonium persulfate (APS, 98%, Merck, Germany), hydrochloric acid (HCl, 37%, Merck, Germany), $TiO_2$ powder (Merck, Germany), ethanol (Merck, Germany), distilled water and deionized water.

### Preparation Method

The method applied was in-situ chemical oxidation polymerization to prepare PANI/$TiO_2$ nanocomposite. The oxidant, ammonium persulfate (APS, $(NH_4)_2S_2O_8$), involved the polymerization from monomer, aniline, in the presence of colloidal $TiO_2$ at room temperature. The 2 mL of colloidal $TiO_2$ from ethanol solution was diluted using 100 mL of deionized (DI) water to yield a transparent solution.

The solution was sonicated for 30 minutes to form a homogenous solution. In another preparation, 1 mL of aniline was dissolved in 200 mL of 2 M hydrochloric acid to mix with the sonicated colloidal $TiO_2$ solution and form a composite solution. For the polymerisation stage, the APS was slowly added dropwise to the composite solution with an equal molar ratio to aniline in moderate stirring for 30 minutes until the dark green colour formed. The solution was filtered, and the residual was washed with distilled water until its filtrate was colourless and clear. The collected green yield was dried in the oven at 60°C for 2 hours. The dried powders were then pressed into pellets. The composite powders were prepared using various amounts of aniline (percentage by the mass fraction of 20, 25, 30, 35, and 40 wt.%) with $TiO_2$.

The performance of the developed composite was tested using a sensing measurement unit by flowing the acetone vapor through the heating chamber. The pellet was pre-heated by flowing air to remove moisture and contaminants in the composite. The sensing activity was conducted at room temperature and atmospheric pressure in a closed vessel. The electrical resistance was recorded on a computer using LabVIEW software via the GPIB interface connected to the electrometer (Keithley 6517A, USA). The performance of the composite was observed through a percentage of the sensitivity

measurement by representing the relation of the electrical resistance of the pellet in the air ($R_A$, Ohm) and in acetone vapor ($R_V$, Ohm), $\Delta S = (R_A - R_V)/R_A$.

## Characterization Methods

Surface morphology of the composite pellet was conducted using a field-emission scanning electron microscope (FESEM, Zeiss Leo Supra 50 VP Field Emission) and transmission electron microscopy (TEM, Philips electron microscope-CM12 (Philips, Netherlands)). The crystallite size of the composite was measured using x-ray diffraction (XRD, Philips PW1710), while the composite porosity was measured using $N_2$ adsorption-desorption BET analysis (Autosorb 1-C). The existence of a functional group that forms bonding in the composite was observed through Fourier transform infrared (FTIR, IR Prestige-21 FT-IR Shimadzu) analysis and the type of isotherm for absorbent-absorbate interaction.

## RESULTS AND DISCUSSION

### Structural Nanocomposite Analysis

The surface of the developed PANI-TiO$_2$ nanocomposite was analyzed using different characterization analyses. Figure 2 shows FESEM and TEM images for pure PANI and different loadings of PANI into TiO$_2$ structure, which are 20, 30, and 40 wt.%. From images, the pure PANI shows blurry images without clear boundaries due to the amorphous structure of the polymer. Meanwhile, the loadings of PANI into TiO$_2$ particles maintain a good crystallite structure because TiO$_2$ has good crystallinity. For lower loadings of PANI, which is 20 wt.%, the PANI is distributed among TiO$_2$ particles, and the size of TiO$_2$ is not affected as much. From XRD measurement, the crystallite size is 18.55 nm compared to the pure TiO$_2$, which is 38.45 nm. The TEM images also show that PANI's existence is almost invisible, probably due to small loadings.
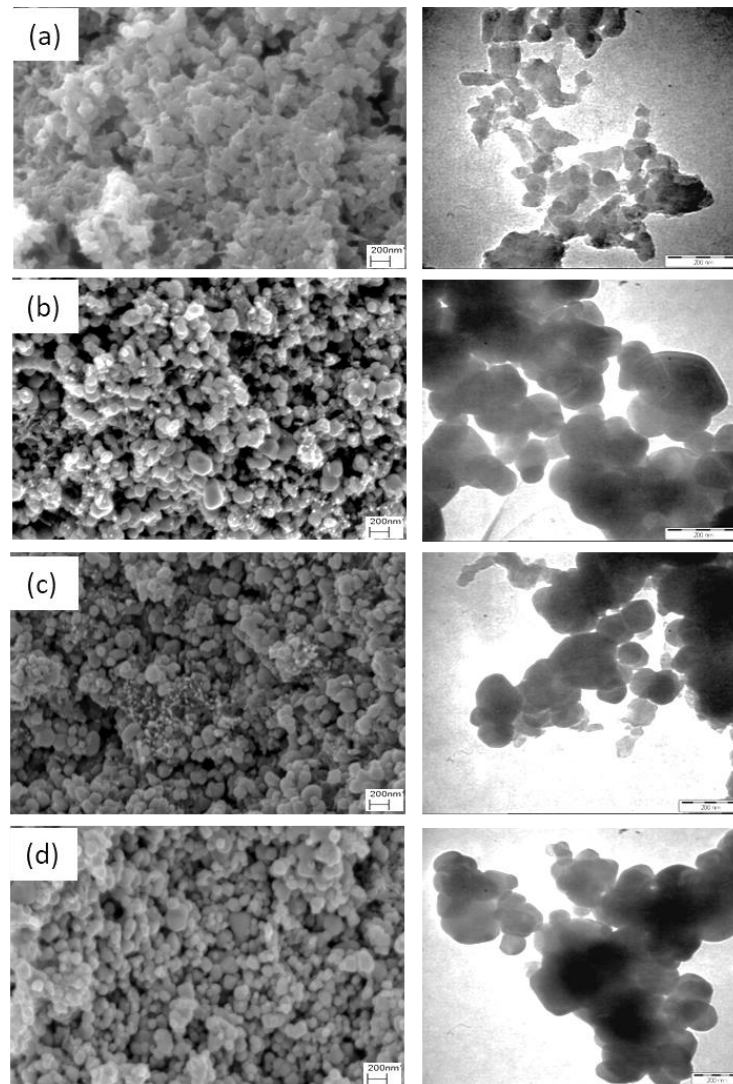


**Figure 2.** FESEM analysis (left) and TEM analysis (right) for various PANI loadings of (a) pure PANI, (b) 20 wt.%, (c) 30 wt.%, (d) 40 wt.%.

When further increasing the PANI addition to 30 wt.%, the PANI seems to form few agglomerations with TiO$_2$. The TEM images represented the blurry PANI between TiO$_2$ particles and well-dispersed within the formation. The crystallite size of 30 wt.% PANI loadings is 25.34 nm, the same as 20 wt.% loadings where the size is less than the pure TiO$_2$ particle. The small size is essential to provide a larger surface area for particle reaction when exposed to the vapour during detection. The small size-to-volume ratio will improve the composite stability and sensing activity [13]. The increment towards 40 wt.% shows that the agglomerations of particles turn bulky in size, as presented in TEM images. The crystallite size gives the measurement of 48.73 nm, which is larger than pristine TiO$_2$ and probably due to a higher tendency on agglomeration formation for higher loadings of PANI. The role of PANI within this range of percentage of loadings gives an overview of sufficient loadings of PANI to provide good adsorption and desorption processes.

The interaction between PANI and TiO$_2$ was further analyzed through FTIR to observe the bonding involved from the existing functional group. The profiles of PANI loadings were almost the same as the pure PANI for a range of 1,000 to 1,600 cm$^{-1}$, where significant bonding exists between PANI and TiO$_2$, as shown in Figure 3. The peaks at 1,489 cm$^{-1}$ of pure PANI represented C=N (quinonoid). The peak at 1,504 cm$^{-1}$ represented C=C (benzenoid) bonds in PANI loadings, while C-N aromatic amines were at the band of 1,300 cm$^{-1}$ [14]. The band of 1,141 cm$^{-1}$ for PANI loadings is assigned to the vibration mode of the –NH$^+$ = structure that is related to the charged polymer unit of Q=NH$^+$−B or B−NH$^{+\bullet}$−B [18]. The bands are larger when the PANI loadings are increased due to the stronger bond of the elements in the polymer unit. The band of 1,141 cm$^{-1}$ also gives input on the degree of electron delocalization and composite electrical conductivity. The peak intensity increases compared to pure PANI, which shows that adding PANI can provide effective electron delocalization. The interaction between PANI loadings with TiO$_2$ was shown through the bonding of O-H at a broad spectrum of 3,464 cm$^{-1}$, and it is cleared for 30 wt.% loadings compared to 20 and 40 wt.%. A strong bonding is formed between the elements during composite formation [15].

The good bonding of the composites shows that the PANI loadings in TiO$_2$ significantly affect the materials' collaborations. Another important measurement of a successful adsorption process is the porosity of the materials or composite. The BET surface area of the pure TiO$_2$ was 7.26 m$^2$/g, and the average pore diameter was 25.90 nm. After the addition of PANI, the BET surface area measured a larger increment to 18.44 m$^2$/g and 14.67 m$^2$/g for 30 wt.% and 40 wt.%, respectively. Meanwhile, there is a small increment of 20 wt.%; the surface area is 9.53 m$^2$/g, resulting in a larger pore diameter of 36.64 nm. The average pore diameter of 30 wt.% is smaller, 23.14 nm, due to good particle contact and distribution in the composite, while the addition of 40 wt.% PANI forms a bulky structure (pore diameter of 50.50 nm) with larger agglomeration. This condition will reduce the efficiency of the adsorption process and make it difficult to desorb vapor due to a higher tendency for clogging formation [9-10]. The slower adsorption process will affect unstable detection with minimum sensitivity towards acetone vapor. Therefore, the 30% PANI-TiO$_2$ composite has higher specific surface areas and porous structures, which benefit the enhancement of sensing performance. Furthermore, they provide more active sites and adsorb more reactive species.
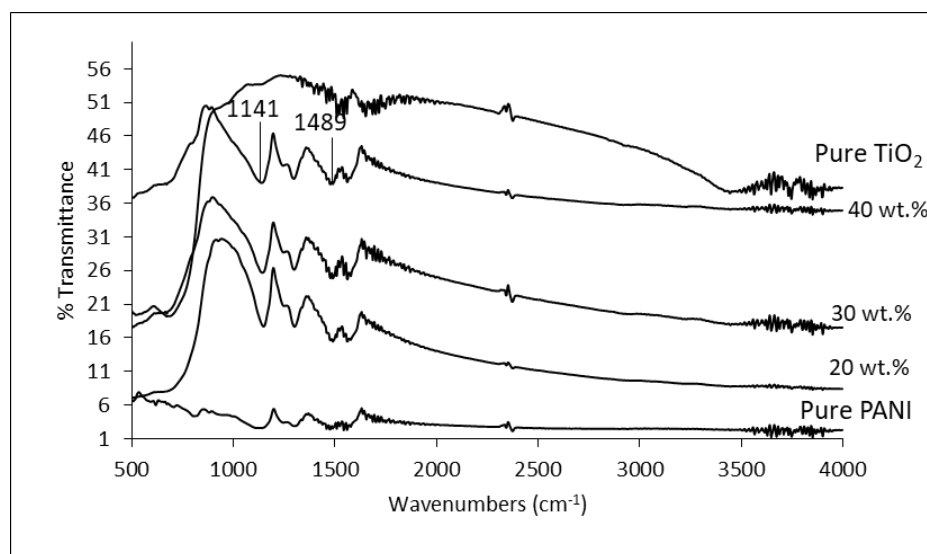


**Figure 3.** FTIR analysis of pure TiO$_2$, pure PANI, and different PANI loadings of 20 wt.%, 30 wt.%, and 40 wt.%.

## Acetone Sensing Performance and Optimization

The performance of the PANI-TiO$_2$ nanocomposite is verified through the effect of operating temperature and acetone vapor concentration. Initially, the stability of the nanocomposite was observed by flowing air through the measurement unit, and it was found that the 20 wt.% PANI-TiO$_2$ has good stability with a value of log R higher than pure TiO$_2$ as the temperature increases, as shown in Figure 4 (a). The reading of pure TiO$_2$ was $10^{12}$ $\Omega$ and largely decreased to $10^5$ $\Omega$ after the addition of PANI. The charge between electrons was effectively transferred in the nanocomposite within the temperature range, and the materials had good thermal stability. However, the measurement is not consistent for this percentage of composition. Thus, the measurements for other percentages were optimized.

The sensitivity of the materials is an important factor during sensing activity. Figure 4 (b) shows the comparison of sensitivity measurement between pure TiO$_2$ and 20 wt.% of PANI. It showed that the nanocomposite PANI-TiO$_2$ has good stability when the temperature increases during electrical measurements. The reading of percentage sensitivity was a maximum temperature of 45°C and decreased at higher temperatures. Therefore, the addition of PANI can lower the operating temperature with good performance compared to pure TiO$_2$, which is limited to performing at very low temperatures [12]. Meanwhile, for the effect of acetone vapor concentration, the measurements for both materials almost have the same profile but only show maximum

percentage sensitivity at a concentration of 350 ppm. From this measurement, the addition of PANI shows significant changes in acetone detection, which needs to be optimized for other PANI loadings.

## Optimization of Sensing Activity

The optimization of different PANI loadings was conducted using the response surface method using Design of Experiment (DOE) software to analyse the interaction between parameters was observed. Figure 5 shows one factor of the interaction profile for parameters of percentage nanocomposite, operating temperature, and concentration of acetone vapor. The maximum suggested conditions are PANI loadings of 30 wt.%, temperature of 45°C, and 300 ppm of acetone concentration. This analysis was based on measurements collected from the experiment and analysed through ANOVA analysis. From the F-test study, the interaction between temperature and acetone concentration gave a significant response towards sensitivity and suggested eliminating the less affecting response, which is the PANI loadings. The effect on the 45 to 55°C range has a larger percentage sensitivity than acetone concentration. Therefore, the analysis suggested the optimum detection condition was at 45°C and 300 ppm concentration. The 30 wt.% of PANI loadings were tested again and operated at the suggested optimum condition. The sensitivity percentage was obtained at 16.19% through this condition, and the error was very minimal compared to that predicted by the analysis, which is a 0.02% error.
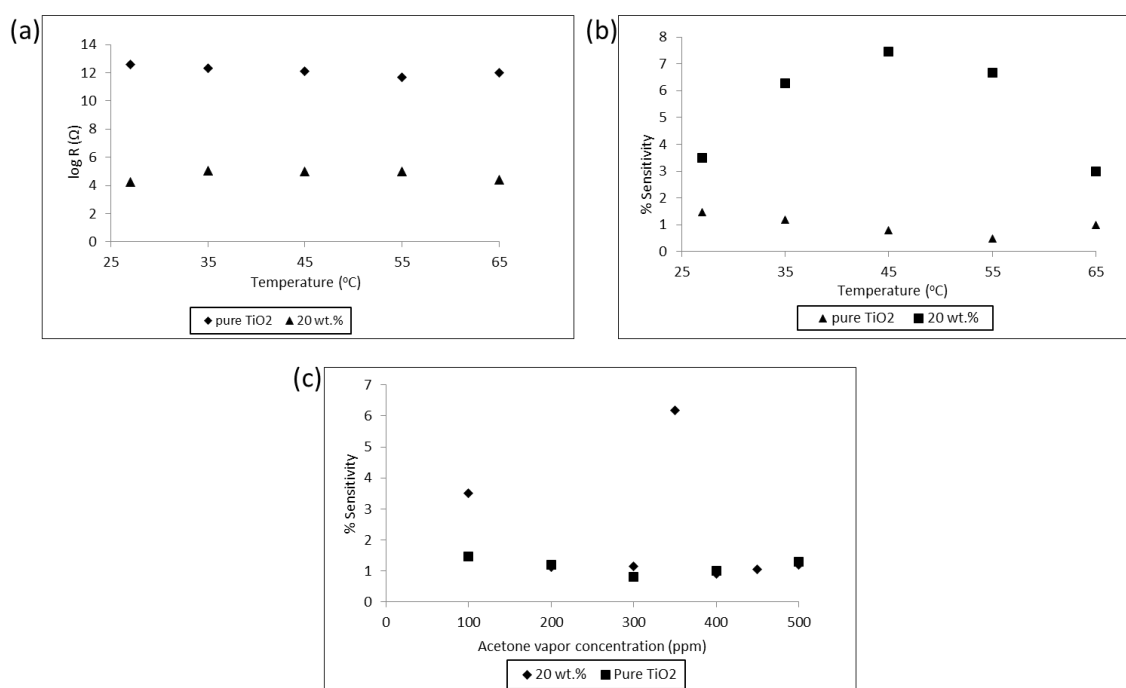


**Figure 4**. Measurement of (a) electrical resistance in purified air, (b) effect of operating temperature, (c) effect of acetone vapor concentration for pure TiO$_2$ and PANI loadings of 20 wt.%.
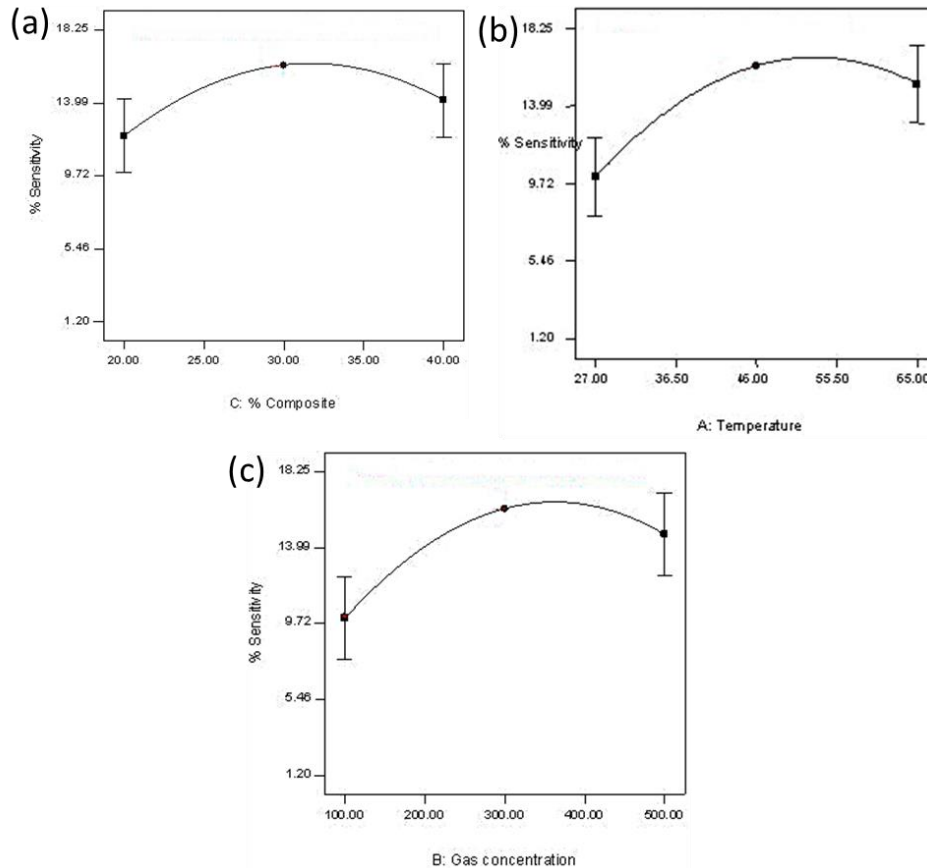
**Figure 5.** The effect of important parameters (a) the percentage of the nanocomposite, (b) temperature, and (c) acetone vapor concentration on percentage sensitivity during acetone detection.

Therefore, adding PANI improved the material structure from pure $TiO_2$, eventually enhancing the adsorption-desorption process in the sensing activity [6]. The larger surface area of 30 wt.% PANI loadings gives good reflection towards detection by providing a larger active area for the adsorption of oxygen species, and the desorption process is smooth due to the good sensitivity of the nanocomposites.

## CONCLUSION

The PANI-$TiO_2$ nanocomposite was successfully prepared using in-situ chemical polymerization method for various percentage compositions (20 – 40 wt.%). From characterization analysis of the nanocomposite, the loadings PANI of 30 wt.% showed good complementation for the adsorption process where the surface area measured is 18.44 $m^2/g$ compared to pure $TiO_2$ without adding PANI. The average pore diameter is also very minimal to provide a process of adsorption-desorption of acetone sufficiently. From the sensing activity, the addition of PANI improved detection at lower temperatures, and the optimum operating condition was obtained at 45°C and 300 ppm acetone vapour concentration. The reading of sensitivity was at 16.19%, while compared to pure $TiO_2$, it only can have a very low sensitivity of

1 to 2% sensitivity. The sensitivity of the PANI-$TiO_2$ nanocomposite is decreased for higher than 45°C due to the lower effectiveness at higher temperatures and bulky particles that will provide a slower adsorption process. This study concluded that the findings provide surface structure information of organic-inorganic gas sensors for detection at lower temperatures that are suitable for safety precautions on the gas leaking issue in the industrial and research sectors.

## ACKNOWLEDGEMENT

## REFERENCES

1.   Wang, J., Li, Z., Zhang, S., Yan, S., Cao, B., Wang, Z. and Fu, Y. (2018) Enhanced $NH_3$ gas-sensing performance of silica modified $CeO_2$ nano-structure based sensors. *Sensors and Actuators B: Chemical*, **255**, 862–870.

2.   Zhang, D., Yang, Z., Wu, Z. and Dong, G. (2019) Metal-organic frameworks-derived hollow zinc oxide/cobalt oxide nanoheterostructure for highly

sensitive acetone sensing. *Sensors and Actuators B: Chemical*, **283**, 42–51.

3.  Wang, Y., Wu, T., Zhou, Y., Meng, C., Zhu, W. and Liu, L. (2017) TiO$_2$-Based Nanohetero-structures for Promoting Gas Sensitivity Performance: Designs, Developments, and Prospects. *Sensors*, **17(9)**.

4.  Jumali, M. H. H., Izzuddin, I., Najib, H., Yahaya, M. and Salleh, M. M. (2011) Ethanol sensing behaviour of TiO$_2$-PVK Thin films. *Solid State Science And Technology*, **19(2)**, 8–15(2).

5.  Hossain, M. K., Hendi, A., Asim, N., Alghoul, M. A., Rafiqul Islam, M. and Hussain, S. M. S. (2023) Chemiresistive Gas Sensing using Graphene-Metal Oxide Hybrid. *Chemistry – An Asian Journal*, e202300529.

6.  Mofdal, M. E. E., Al-Hazeem, N. Z., Ahmed, N. M. and Al-Hardan, N. H. (2022) Amperometric room temperature hydrogen gas sensor based on the conjugated polymers of polypyrrole–poly-ethylene oxide nanofibers synthesised via electro-spinning. *Journal of Materials Science: Materials in Electronics*, **33(9)**, 7068–7078.

7.  Kashyap, R., Kumar, R., Kumar, M., Tyagi, S. and Kumar, D. (2019) Polyaniline nanofibers based gas sensor for detection of volatile organic compounds at room temperature. *Materials Research Express*, **6(11)**, 1150d1153.

8.  Zhang, J., Liu, X., Neri, G. and Pinna, N. (2016) Nanostructured Materials for Room-Temperature Gas Sensors. *Advanced Materials*, **28(5)**, 795–831.

9.  Liu, A., Lv, S., Jiang, L., Liu, F., Zhao, L., Wang, J., Hu, X., Yang, Z., He, J., Wang, C., Yan, X., Sun, P., Shimanoe, K. and Lu, G. (2021) The gas sensor utilizing polyaniline/ MoS$_2$ nano-sheets/SnO$_2$ nanotubes for the room temperature detection of ammonia. *Sensors and Actuators B: Chemical*, **332**, 129444.

10. Aparicio-Martinez, E., Osuna, V., Dominguez, R. B., Marrquez-Lucero, A., Zaragoza-Contreras, E. A., and Vega-Rios, A. (2018) Room Temperature Detection of Acetone by a PANI/Cellulose/WO$_3$ Electrochemical Sensor. *Journal of Nano-materials*, 6519694, 9.

11. Jain, A., Gautam, S. K. and Panda, S. (2023) NH$_3$-detecting room temperature PANI-TiO$_2$-based flexible gas sensor with EIS-validated sensing mechanism. *Physica Scripta*, **98(9)**, 095909.

12. Izzuddin, I., Jumali, M. H. H., Yahaya, M. and Salleh, M. M. (2012) New hybridization approach of titnium organometallic: PANi thin films as room temperature gas sensors. *Sains Malaysiana*, **41(8)**, 1017–1021.

13. Sambaza, S. S., Maity, A. and Pillay, K. (2020) Polyaniline-Coated TiO$_2$ Nanorods for Photo-catalytic Degradation of Bisphenol A in Water. *ACS Omega*, **5(46)**, 29642–29656.

14. Marimuthu, T., K. Sambasevam, S. N. A., Baharin and Jamion, N. A. (2020) Fabrication of Ammonia Gas Sensor Based on Polyaniline/ Mussel Shell Composite. *ASM Science Journal*, **13**, 105–110.

15. El Sammak, A. A., Mohamed, W. A. A., Elnaggar, E. M. and El-Sayed, B. A. (2023) Recycling and photodegradation processes of organic hazardous materials on polyaniline-titanium dioxide quantum dots catalyst. *Egyptian Journal of Petroleum*, **32(3)**, 15–23.